Article

Secondary Network Formation in Epoxidized Natural Rubber with Alternative Curatives

Alexandra Shakun, Noora Kemppainen, and Essi Sarlin*

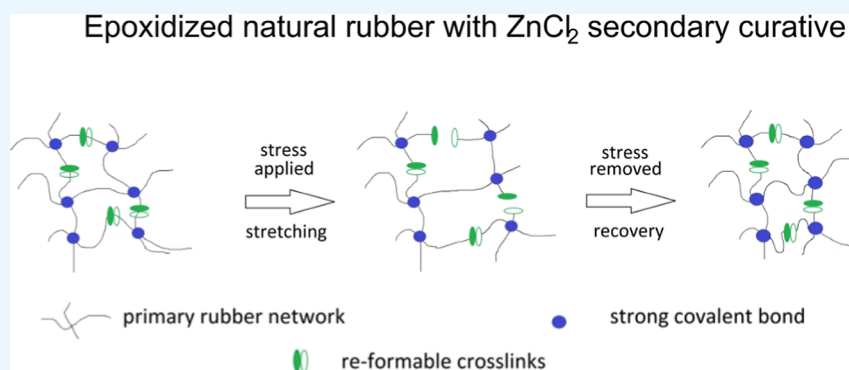Cite This: *ACS Omega* 2024, 9, 36326−36340

Read Online

ACCESS | Metrics & More | Article Recommendations | Supporting Information

Epoxidized natural rubber with ZnCl₂ secondary curative

stress applied / stretching — stress removed / recovery

primary rubber network — strong covalent bond — re-formable crosslinks

ABSTRACT: Epoxidized natural rubber (ENR) offers a unique combination of strength, sustainability, and versatile structure, making it a good candidate for creating sacrificial and reformable bonds via secondary curatives. These curatives should be simple and compatible with other rubber ingredients and industrial mixing processes. Although many alternative curatives, including zinc chloride, zinc dimethacrylate (ZDMA), and sebacic acid (SA), have been proven to be successful, they have never been compared in the same compound. Moreover, the effectiveness of these alternative curatives on network formation, including their interactions with the other ingredients of a rubber compound, such as fillers, coupling agents, and traditional curatives, has not been fully studied yet. Based on the current study, these secondary curatives alone cannot provide a sufficient level of vulcanization. However, adding ZDMA or SA together with sulfur curatives allowed improving the tensile properties and showed microlevel self-healing behavior during cyclic loading. The addition of 10 phr (parts per hundred rubber) ZnCl₂ created weak, short, and rigid bonds in ENR detectable by simple Payne measurements. However, that led to active interaction with all compounding ingredients and deterioration of the physical properties. Reducing the ZnCl₂ load to 1 phr allowed full recovery of stress after the cyclic test and fair tensile strength of the compound.

INTRODUCTION

Nature has always been an inspiration for material development. Strength and durability improvements in polymeric materials can be inspired by spider silk and natural rubber (NR) latex, which have secondary polymer networks with the ability to bear the stress alongside the main polymer network. With the introduction of sacrificial bonds or a self-healing secondary network, man-made polymeric materials can achieve higher strength, toughness, wear resistance, and an extended lifetime.[1] These changes would actively contribute to the sustainability of consumer rubber goods and technical rubber items[2−4] or achieve advances in robotics and wearable electronics.[5,6] Moreover, some types of sacrificial and reformable bonds could enable easy devulcanization routes, thus making rubber easily recyclable.[7−12] Sacrificial bonds are often described as short and weak compared to the long and flexible polysulfidic bonds dominating the conventional sulfur vulcanization network. Sacrificial bonds are usually noncovalent, for example, hydrogen bonds, coordination clusters, and metal ligands, while self-healing cross-links can also be formed by dynamic covalent bonds that are able to reform at specific conditions. In order to provide additional strength and toughness, sacrificial bonds must be weaker and shorter than the other bonds in the highly stretchable matrix. Thus, when an external force is applied to the material, such bonds would break, first dissipating the energy and keeping the main bonds intact.[11]

A large number of alternative curing chemicals and material combinations have been studied during the past decades, allowing the creation of sacrificial, hybrid, and/or self-healing

networks in rubbers. As revealed by the recent scientific reviews, most research has been focusing both on general rubber types like NR, butadiene rubber, and styrene-butadiene rubber (SBR) vulcanized by sulfur or peroxide and on special grades of elastomers, like nitrile rubber (NBR), epoxidized natural rubber (ENR), halogenated rubbers, and others.[1,13−21] In some cases, nonrubber constituents of NR are utilized to promote self-healing behavior.[22] Among the special types of rubber, alternative cross-linking routes for ENR have gotten a lot of attention from the researchers.[7,23−28] Indeed, ENR has an outstanding entirety of properties and high sustainability: it originates from a natural source, has superior strength and wear properties of NR, is compatible with most general rubber types, improves dispersion of silica filler, reduces the rolling resistance of a tire, thus reducing fuel consumption, and has a structure allowing chemical grafting and modification through various routes.[29−36] The most efficient modification mechanisms of ENR promoting the creation of sacrificial and reformable cross-links include hydrogen bonding, reversible disulfide cross-links, e.g., disulfide metathesis, and ionic interactions.[14,37]

Zinc-based sacrificial networks appear to be comparably common and very relevant for the rubber industry as zinc compounds are already used in conventional curing systems as accelerators and activators. Moreover, as mentioned in ref 38, such networks containing ionic sites are prone to self-healing as well. However, despite the extensive research and known reaction routes between ENR and many alternative curatives, interactions between the elastomer, curative, and other compounding ingredients are usually not taken into account. Considering the presence of highly reactive components, such as silica, a widely used reinforcing filler, a silane coupling agent facilitating the dispersion of silica, and vulcanization accelerators, possible interactions with secondary curatives should affect the compound a lot. This could be the reason why some researchers focus on achieving self-healing only with traditional vulcanization packages, such as sulfur, accelerators, zinc oxide, and stearic acid. For example, Hernández Santana et al.[14] have stated that NR shows a certain degree of self-healing, which is most efficiently created by the semieffective sulfur vulcanization system (semi-EV), meaning that the ratio of sulfur to accelerator is close to one. Continuing the same approach, Araujo-Morera[39] has studied the possibilities of semi-EV systems rich in poly- and disulfidic cross-links and varying amounts of curing ingredients on self-healing of SBR. However, traditional sulfur vulcanization systems alone cannot achieve the full potential of the self-healing and may need to be modified with secondary chemicals. Thus, except for studying the cross-linking possibilities offered by the alternative curatives, it is important to understand the interactions they have with other rubber ingredients. For example, zinc dimethacrylate (ZDMA), in addition to being a curing agent, seems to have a good compatibilizing action on silica in some rubbers without the addition of silane. According to the data presented in ref 40, the addition of ZDMA effectively decreases the Payne effect in uncured hydrogenated NBR compounds. ZDMA alone showed good dispersion in that compound as well; however, its use with carbon black led to more agglomeration of the filler particles. Furthermore, the ENR itself has been extensively studied as a compatibilizer for silica-containing compounds. Owing to the epoxy ring (or −OH groups in the case of ring opening), ENR is able to create hydrogen bonding to the hydroxy groups of the silica surface

and, at the same time, participate in the vulcanization reaction with sulfur as well as undergo self-cross-linking. The addition of ENR has been shown to improve the strength of the material but was not efficient enough to replace the conventional silane agent, such as TESPT.[34]

ENR has also been used to create secondary networks via zinc diacrylate (ZDA) cross-linking in the SBR matrix, resulting in dual vulcanization.[41] There, 10 phr of ENR and 1−4 phr of ZDA were used. The mechanism of curing ENR with zinc diacrylates based on the oxa-Michael reaction was confirmed by a model reaction[42] and was further discussed in the work of Zhang et al.[28] According to Zhang et al., ZDA can serve as a catalyst for the epoxy ring opening reaction and promote the reaction between −OH groups of ENR and the vinyl groups of ZDA. Moreover, metal complex bonds can be created between the Zn^{2+} ion of ZDA and the epoxy rings of ENR. Furthermore, due to the continuous ring opening reaction, ENR cured purely with ZDA is expected to exhibit a marching modulus. If silica is used in compounding, even more pronounced marching curing curves would be observed due to the absorption of ZDA by the silica surface and its gradual release with time. Finally, increased amounts of ZDA significantly shift the glass transition temperature (T_g) of the compounds toward higher temperatures. Except for the organic salts of zinc discussed previously, addition of up to 10 phr $ZnCl_2$ salt[43,44] has been studied as an alternative curative. Although the potential release of Cl^- ions into the matrix is not usually discussed well, the curing of ENR by metal chloride can result in the chlorination of ENR instead of the release of Cl^- ions.[23]

Another type of material capable of effectively curing ENR is dicarboxylic acid.[26] The vulcanization reaction is based on the interaction between the epoxy ring of rubber and the −COOH group of the acid that would happen at high temperatures. Such bonds are expected to be reversible.[45] Another benefit of dicarboxylic acid [for example, sebacic acid (SA)] is the possibility of being produced from a natural source and improving the flexibility of polymers.[46]

The present research is focused on evaluating the potential of different alternative curatives to create relatively weak bonds in ENR and studying how they work in a hybrid network together with a conventional sulfur curing system. Zinc salts (inorganic and organic) and dicarboxylic acids were selected for this purpose. As mentioned above, all compounding ingredients selected for the present study are expected to have interactions with each other; however, the exact routes and mechanisms of such interactions may vary. For example, the selected secondary curatives could form covalent, ionic, and hydrogen bonds, or their combination with ENR. With temperature, pressure, and vulcanization being the same for all compounds, the curing route would be different depending on if ring-opening is happening in ENR and how many other components are in the system. Silica, for example, can adsorb the chemicals onto its surface, and ENR, silanes, and secondary curatives could be competing to interact with the silanol groups. The study is divided into three sections to proceed from very simple compounds to more complex systems and analyze the changes the increase in complexity brings to the performance of secondary curatives and the bonds they create. Moreover, the ways of experimental assessment of such bonds are discussed, for example, the possibility of using Payne effect measurements for the detection and evaluation of secondary networks.
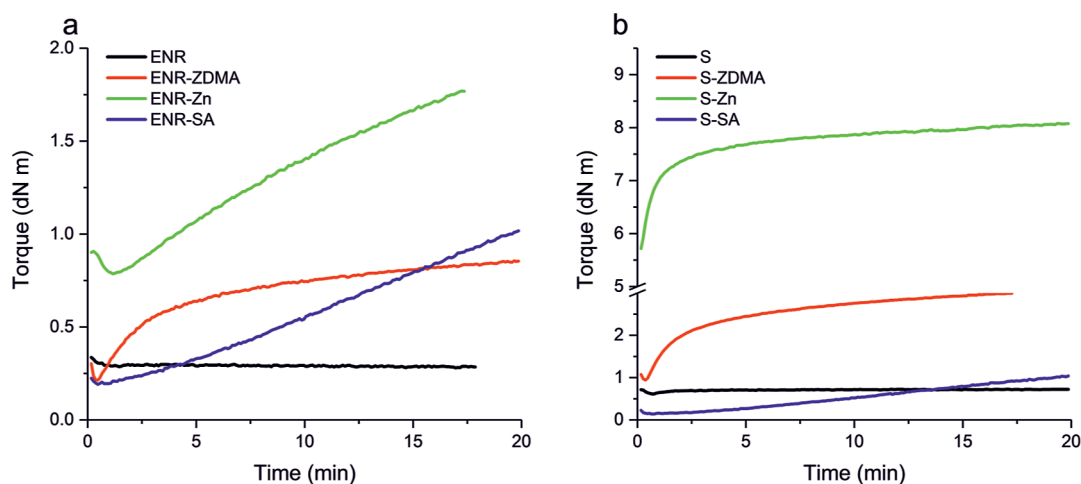
■ EXPERIMENTAL SECTION

Materials. ENR with 25% epoxy group content (Epoxyprene 25, Muang Mai Guthrie PCL) was used in the study along with silica (Zeosil 1165, Solvay Rhodia) and secondary curatives: zinc chloride ($ZnCl_2$, Sigma-Aldrich), zinc methacrylate (ZDMA, Dymalink 708, TotalEnergies Petrochemicals & Refining USA, Inc.), and SA (Sigma-Aldrich). Additionally, 99% elemental sulfur (Esseco S.r.l.) and N-cyclohexyl-2-benzothiazole sulfenamide (CBS, General Quimica) medium fast primary accelerator, both industrial grades, were used in the study. Silane coupling agents for silica included conventional bis[3-(triethoxysilyl)propyl] tetrasulfide (TESPT (Si69), Evonik) and 3-glycidyloxypropyltrimethoxysilane (ES, Dynasylan GLYMO, Evonik). All materials were used as received. The chemical structures of the used materials can be seen in Figure S1 (Supporting Information).

Compound Preparation. The compounds contained 100 phr (parts per hundred rubber) of ENR, 30 phr of silica, 3 phr of coupling agent, 10 phr of secondary curatives (unless marked otherwise), 1.45 phr of sulfur, and 1.8 phr of CBS. The sample designated as ENR contains only 100 phr of ENR without any other additives. The exact ingredient contents of the compounds and their designations are shown in Table 1. Compounding was done at a 50 cm^3 Brabender internal tangential mixer with a fill factor of 0.73. The mixing started at 80 °C and 60 rpm. ENR was masticated for 45 s, then half of silica with silane was added, followed by the rest of silica and then secondary curatives. The total mixing time of the first stage was 4 min. Silanization was performed as a separate mixing step with a start temperature of 120 °C at 50 rpm and a maximum end temperature of 150 °C to promote the reaction between silica and the coupling agent and facilitate filler dispersion. Conventional curatives were added in a separate mixing step starting at 50 °C and 50 rpm with a total of 3 min mixing and a maximum temperature of 80 °C to avoid premature vulcanization. As the samples containing 10 phr of $ZnCl_2$ were challenging to mix and obtain good quality samples, the amount of $ZnCl_2$ was decided to be decreased to 0.5, 1, and 2 phr. The resulting compounds are designated as C-Znx and S-Znx for samples with and without conventional curatives, respectively, where x is the amount of $ZnCl_2$ in phr. The compounds were cured into 2 mm sheets in a hydraulic press (20 bar) at 160 °C. The vulcanization time was $(t_{90} + 2)$ minutes, where t_{90} is the time when 90% of maximum rheological torque was achieved. In cases where rheologic curves had no torque increase or showed marching, the maximum rheologic torque or optimum vulcanization time t_{90} could not be achieved, and such samples were cured in a press for 20 min. The visual appearance and transparency of samples are shown in Figure S2.

Characterization. The curing parameters of the samples were determined with the parallel plate die rheometer (APA 2000, Alpha Technologies) at 160 °C. The Payne effect was measured with the same equipment at 100 °C and 0.5 Hz frequency when the angular strain was stepwise increased from 0.28 to 140.2%, and the shear modulus G' was obtained. The Payne effect is reported as a change in shear modulus ($\Delta G'$) from maximum modulus value (G'_{max}) to minimum modulus value (G'_{min}). Although conventionally, the Payne effect is determined from filled unvulcanized samples and aims to describe the filler−filler network in the compound, also unfilled samples and samples cured with only secondary curatives were

Table 1. Content and Designation of Compounds

designation	group B (bicomponent)				group S (filled ENR with secondary curatives)												group C (filled ENR with secondary + conventional curatives)							
ingredient	ENR-Zn	ENR-ZDMA	ENR-SA	ENR	S	S/Si69	S/ES	S-Zn	S-Zn/Si69	S-Zn/ES	S-ZDMA	S-ZDMA/Si69	S-ZDMA/ES	S-SA	S-SA/Si69	S-SA/ES	C	C/Si69	C-Zn	C-Zn/Si69	C-ZDMA	C-ZDMA/Si69	C-SA	C-SA/Si69
ENR	x	x	x	x	x	x	x	x	x	x	x	x	x	x	x	x	x	x	x	x	x	x	x	x
silica					x	x	x	x	x	x	x	x	x	x	x	x	x	x	x	x	x	x	x	x
TESPT						x			x			x			x			x		x		x		x
ES							x			x			x			x								
ZnCl$_2$	x							x	x	x									x	x				
ZDMA		x									x	x	x								x	x		
SA			x											x	x	x							x	x
S + CBS																	x	x	x	x	x	x	x	x

Figure 1. Curing curves of simple compounds (a) without silica and (b) with silica.

analyzed in the present work. Here, in the unfilled compounds, the Payne effect measurement is suggested to evaluate the presence of weak sacrificial networks. Secondary curatives are assumed to contain chemical groups that are able to form hydrogen bonds with ENR and establish a weak network resembling the filler network in the conventional uncured compound. In this case, both cured and uncured compounds containing only secondary curatives (group B) were tested to confirm that curing in press, not solely mixing, is responsible for the network formation. Furthermore, testing the Payne effect of silica-filled compounds containing only secondary curatives (group S) allows us to evaluate the role the filler plays in the formation of the mentioned secondary network. Thus, Payne effect measurement is expected to be a useful tool to visualize the presence of a weak sacrificial network in the sample as well as evaluate the effect of the compounding ingredients and network formation parameters on it.

Tensile testing was performed on an Instron 5967 universal tester with a 500 N load cell using a dumbbell specimen (ISO 37 type 3) with a 10 mm test length at a 500 mm/min rate. The reinforcement index (RI) was calculated as a ratio of stress at 300% elongation (M_{300}) to stress at 100% elongation (M_{100}). The tensile cyclic loading was performed with the same equipment at ambient conditions at a 500 mm/min rate for 4 mm-wide rectangular test samples with a test length of 25 mm and a maximum elongation of 200%, and the stress at maximum elongation (M_{200}) of each cycle was recorded. After the first 5 cycles, the samples were kept in ambient conditions and cyclically tested again after 24 h. The same samples were placed in an oven at 50 °C for 1 h, and the final cyclic testing was done. Three samples per compound were tested, and the average was calculated. The recovery percent was calculated as the ratio of regained stress M_{200} after conditioning to the stress loss between the first and last cycles of the initial test

$$R\ \% = \frac{M_{c1} - M_{i5}}{M_{i1} - M_{i5}} \times 100,\ \%$$

where M_{iy} is M_{200} of the initial cyclic test, M_{cy} is M_{200} of the conditioned sample, and y is the number of the cycle.

Fourier transform infrared spectra (FTIR) were obtained with PerkinElmer spectrum two in the attenuated total reflectance mode in the range of 600 to 4000 cm^{-1} with a diamond crystal background and 4 cm^{-1} resolution. Selected samples were polished with argon at −50 °C by the JEOL

Cooling Cross Section Polisher IB-19520CCP and studied with a scanning electron microscope (Zeiss ULTRAplus) equipped with an energy-dispersive X-ray spectroscopy detector (Oxford Instruments X-MaxN 80). The samples were coated with a thin carbon layer to prevent charging during the SEM analysis. Thermogravimetric (TGA) data was obtained with TG 209 F3 Tarsus (Netzsch) in N$_2$ gas flow. The samples were heated to 600 °C at a 10 K/min rate. The glass transition and the presence of secondary curatives were studied by means of differential scanning calorimetry (DSC) with DSC 214 Polyma (Netzsch) in N$_2$ gas flow with 10 K/min heating and cooling rates.

The apparent cross-link density (1/Q) was calculated for 1 × 1 cm samples immersed in toluene in closed vessels for 72 h and then dried for 48 h based on the equation modified from[36]

$$\frac{1}{Q} = \frac{1}{\left(\frac{m_s - m_d}{m_d - m_0 \times \frac{f}{F}} \right)}$$

where m_s and m_d are the weights of the swollen and dried specimens, respectively, m_0 is the initial weight of the specimen, f is the solid particle/filler amount in phr, and F is the total formula weight in phr. Toluene was renewed every 24 h during the measurement. Three parallel samples were used. The modification of the original equation was necessary due to the high dissolution of the sample related to generally low amounts of cross-links created. When dissolution was neglectable, the presented equation was equal to the original equation $1/Q = 1/\left(\frac{m_s - m_d}{m_0} \right) \frac{F}{100}$. The amount of dissolved polymer during the swelling test is calculated based on the equation $D\ \% = 100 - 100 \times \left(m_d - \frac{m_0 \times f}{F} \right) / \frac{m_0 \times 100}{F}$.

■ RESULTS AND DISCUSSION

Secondary Curatives in Simple Compounds. The ability of secondary curatives alone to vulcanize ENR was investigated in this section. Moreover, it was determined that no pronounced self-vulcanization is happening in ENR at the given time and temperature conditions, which can be seen from the curing curve (Figure 1a) and apparent cross-link density data (Table 2). The maximum torque values S'_{max}, relating to compound stiffness, stayed low, and there was

Table 2. Apparent Crosslink Density and Rheologic Curve Parameters of Simple ENR Compounds

sample	$1/Q$, g/g	D %, %	$\Delta S'$, dN m	S'_{max}, dN m
ENR	0.018 ± 0.001	75.2 ± 1.4	0.10	0.34
ENR-ZDMA	0.069 ± 0.001	17.3 ± 0.4	0.64	0.86
ENR-Zn	0.248 ± 0.005	11.2 ± 0.6	0.99	1.77
ENR-SA	0.176 ± 0.003	5.2 ± 0.2	0.85	1.02
S	0.095 ± 0.004	47.9 ± 0.9	0.32	0.85
S-ZDMA	0.223 ± 0.011	9.4 ± 0.8	2.13	3.07
S-Zn	0.271 ± 0.065	17.8 ± 10.9	4.71	5.26
S-SA	0.174 ± 0.019	11.8 ± 3.5	2.69	3.24

almost no increase in torque ($\Delta S'$) was seen, meaning no cross-links were being created during the curing period. Small apparent cross-link density and not full dissolution of the sample in toluene could be related to marginal self-cross-linking via epoxy-ring opening, which is unlikely without sufficient heat and a catalyst, but rather to the presence of hydrogen bonds between epoxy groups.

Meanwhile, ENR-Zn, ENR-ZDMA, and ENR-SA compounds showed some curing behavior along with marching modulus, especially for ENR-Zn and ENR-SA, making it difficult to determine the appropriate time of vulcanization as the torque plateau could not be reached. In the case of samples with added silica (Figure 1b), more active curing behavior and less marching were seen for S-ZDMA and S-Zn, and all the compounds had an increase in minimum torque related to the hydrodynamic effect of filler. The curing curves were in good agreement with the apparent cross-link density data, indicating that ZnCl$_2$ was the most active and SA the least active among the secondary curatives. It also could be seen that S-Zn samples had a high deviation from the results due to the poor dispersion of zinc salt that was visible in the samples as large particle agglomerates compared to the other S-type samples (Figure S2). Finally, the low torque values of the S-SA sample suggested that SA could have a compatibilizing effect toward silica and the ability to disintegrate silica networks, thus reducing the stiffness of the compound, as later confirmed by the Payne effect measurements presented in Table 3 and Figure 4.

Table 3. Payne Effect Values for the Simple Compounds

sample	uncured		cured	
	$\Delta G'$, kPa	G'_{min}, kPa	$\Delta G'$, kPa	G'_{min}, kPa
ENR	11.5	15.1	9.9	10.8
ENR-ZDMA	9.3	8.5	17.8	30.0
ENR-Zn	19.9	19.6	65.8	44.3
ENR-SA	58.6	15.3	104.6	73.0
S	43.6	14.6	46.5	13.7
S-ZDMA	53.2	15.9	136.5	62.5
S-Zn	178.1	71.8	249.6	182.9
S-SA	12.3	8.8	14.4	38.9

Although Payne effect measurements are usually used to access filler—filler interactions in rubbers, they can be a useful tool for analyzing weak networks. For example, uncured ENR-Zn showed some Payne effect (Figure 2a), as ZnCl$_2$ can also be viewed as a filler forming a network inside the matrix due to hydrogen bonds and ionic interactions. When strain increases, these short and weak bonds break, resulting in a decrease of

shear modulus G'. However, when cured ENR-Zn is tested (Figure 2b), the Payne effect increases significantly from $\Delta G'$ of 19.9 to 65.8 kPa (Table 3), and the minimum modulus G' of cured ENR-Zn is 33.5 kPa higher than that of ENR, implying that a stronger "filler"-rubber network was created in the polymer. In two-component simple systems (sample group B), this Payne effect behavior can be explained by the creation of weak and stiff rubber—zinc bonds that are being broken upon increasing strain. Similarly, an ever stronger effect was visible for ENR-SA samples with a 46.0 kPa increase in $\Delta G'$ due to curing, which can be related to active interaction and weak bond creation between epoxy- and carboxyl-groups. Such an effect was not seen for ENR-ZDMA.

The effect of the secondary curatives on ENR was further studied by FTIR. For example, the new peaks related to the secondary chemicals and the presence of new interactions were seen (Figure 3). First, it was important to determine whether the reaction between ENR and secondary curative was more possible through the epoxy-ring opening reaction, ionic interaction, or some other mechanism. The presence of NR polymer units could be seen from characteristic C = C stretching around 1660 cm^{-1}, CH$_3$ deformation at 1376 cm^{-1} and CH olefin wagging at 842 cm^{-1}.[47] The epoxidation was seen through peaks at about 1250 and 870 cm^{-1}, which are related to the stretching vibration of C—O—C and the oxirane ring itself, respectively. For ENR-Zn, ring opening was expected to be dominant due to the characteristic epoxy ring-related 870−872 cm^{-1} peak disappearance upon curing. As the epoxy ring-related peaks around 1248 and 872 cm^{-1} were present, but shifter toward lower wavelengths, 1241 and 870 cm^{-1}, in the cured ENR-ZDMA and ENR-SA samples, the epoxy ring stayed largely intact, and other types of reactions rather than ring opening must be responsible for the vulcanization of ENR. Another common change in the spectra of ENR upon the addition of secondary curatives was the disappearance of the clear peak at 1540 cm^{-1}, most likely of amide bond from proteins (nonisoprene constituents of the rubber).[48] Its disappearance may be related to the presence of secondary curatives during vulcanization, when the bond between the rubber and protein could have been broken. Furthermore, with the addition of ZDMA to ENR, a peak at 1710 cm^{-1} related to C=O and 1644 cm^{-1} from C=C of metal acrylate appeared in the spectrum indicating the presence of ZDMA, but according to previous works,[39,49,50] an expanded peak around 1540−1550 cm^{-1} may be a sign of C−O···Zn^{2+} interaction, which potentially could mean not only the presence of ZDMA, but an interaction between the epoxy ring and ZDMA. Finally, from the addition of SA, new peaks related to both C=O of ester (1695 cm^{-1}) and the carboxyl group (1730 cm^{-1}) of the ENR-SA compound emerged together with ester stretching (1116 cm^{-1}), and a C−O bond-related peak at about 960 cm^{-1}, indicating that SA was not fully consumed in the curing process and was partly transformed to ester. This, with no evidence of epoxy ring opening, may mean that SA reacts partly with impurities of ENR. The shift of the epoxy group-related peaks nevertheless indicated some weak interaction between the epoxy ring and the secondary curative.[28,51,52] As suggested by Pire et al.,[26] ring opening of ENR and a complete reaction with SA can require higher temperatures, e.g., 180 °C, and hours or vulcanization.

Effect of Silica in Simple Compounds. The addition of silica to compounds is usually expected to increase the Payne effect. The increase was seen for all uncured compounds except
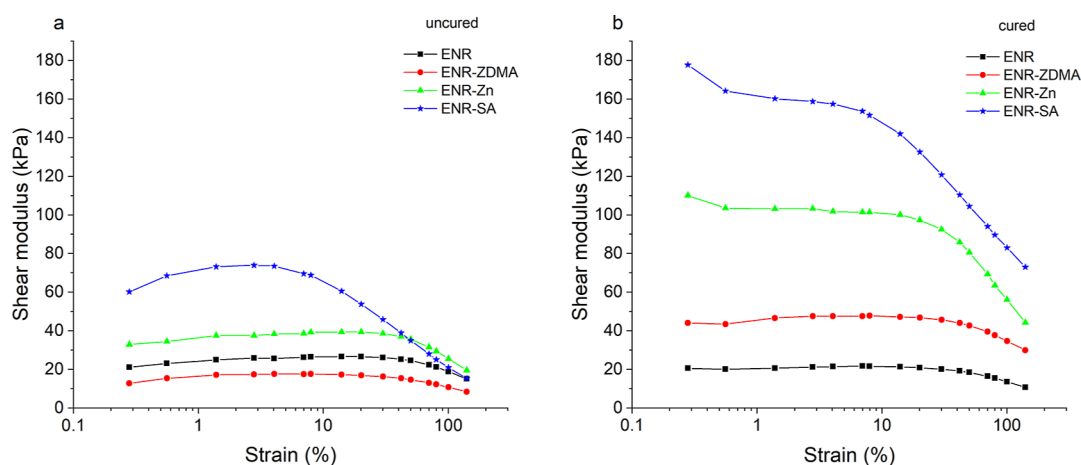
Figure 2. Payne effect curves of (a) uncured and (b) cured simple ENR compounds.
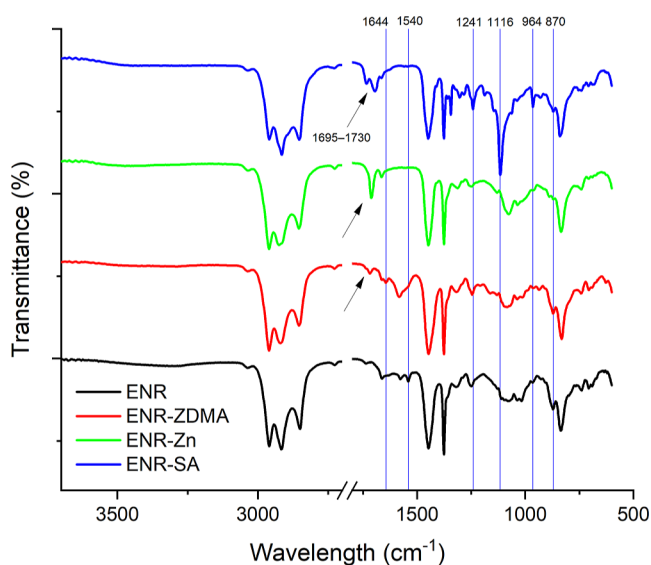

Figure 3. FTIR curves of the simple compounds without silica.

for S-SA, as shown in Table 3 and Figure 4a. The possible explanation is that SA could become adsorbed to the surface of silica and prevent filler network formation, thus causing a significantly low Payne effect. Even for the cured S-SA sample

(Figure 4b), the Payne effect was low, and the small overall increase in shear modulus could be related to the enhanced filler−polymer and polymer−polymer interactions through the introduction of cross-links. A comparison of Figures 4a and 2a would suggest that ZnCl$_2$ interacts more readily with silica than with ENR, but in contrast to SA, it also contributes to filler network formation, potentially through the introduction of ionic bonds, thus increasing the Payne effect. As can be seen from Figure 4b, the Payne effect of the cured S sample was relatively low compared to that of the other samples in the group, which is unusual for silica-filled rubber without silane. ENR is known to have compatibilizing action toward silica due to the presence of oxygen-containing epoxy groups that interact with OH− groups on the silica surface and reduce filler−filler interaction, thus promoting filler dispersion without additional chemicals. This was supported by the decrease in T_g upon the addition of silica (Table 4), which could be related to the reduction of hydrogen bonds between polymer chains and better chain mobility. An increase in the Payne effect of cured S-Zn and S-ZDMA samples could be related to the created network of weak interactions, for example, ionic or hydrogen, not only with silica but with ENR too.

The analysis of mechanical properties (Table 4) revealed that secondary curatives alone were not able to provide sufficient mechanical properties in pure ENR, but ENR-SA
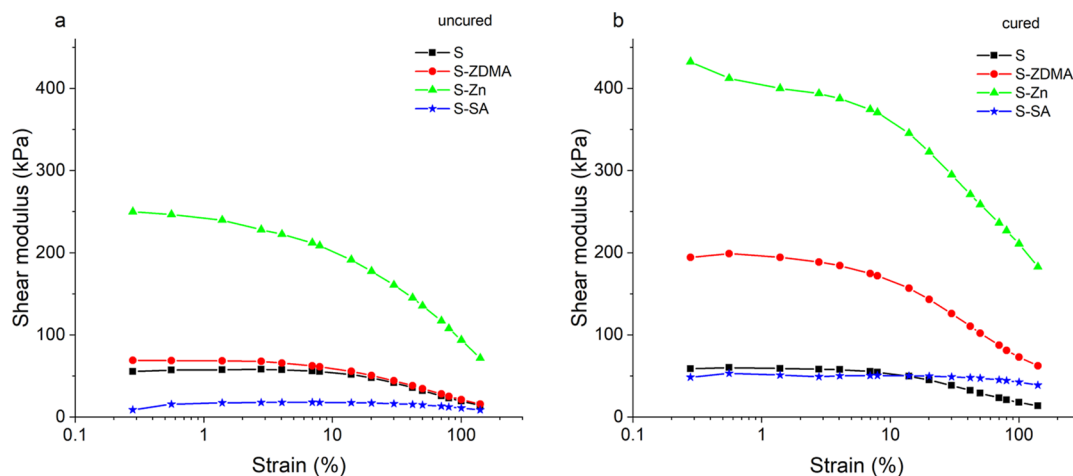

Figure 4. Payne effect of (a) uncured and (b) cured simple ENR compounds containing silica.

Table 4. Mechanical and Thermal Properties of Simple ENR Compounds

sample	T_s, MPa	E_b, %	M_{100}, MPa	M_{300}, MPa	RI, —	T_g, °C
ENR	0.37 ± 0.01	455.7 ± 72.5	0.31 ± 0.02	0.33 ± 0.02	1.08	−41.9
ENR-ZDMA	0.73 ± 0.67	400.9 ± 53.6	0.41 ± 0.00	0.60 ± 0.03	1.48	−41.8
ENR-Zn	1.21 ± 0.02	227.0 ± 33.0	0.78 ± 0.09			−36.9
ENR-SA	2.14 ± 0.34	493.6 ± 62.8	0.65 ± 0.02	1.18 ± 0.06	1.83	−40.1
S	4.23 ± 0.40	512.1 ± 26.3	0.85 ± 0.03	2.35 ± 0.16	2.77	−43.0
S-ZDMA	5.21 ± 1.75	231.0 ± 68.2	2.36 ± 0.82			−39.5
S-Zn	2.66 ± 0.10	98.5 ± 1.1				−31.4
S-SA	5.77 ± 1.72	269.9 ± 44.8	2.23 ± 0.36			−40.5
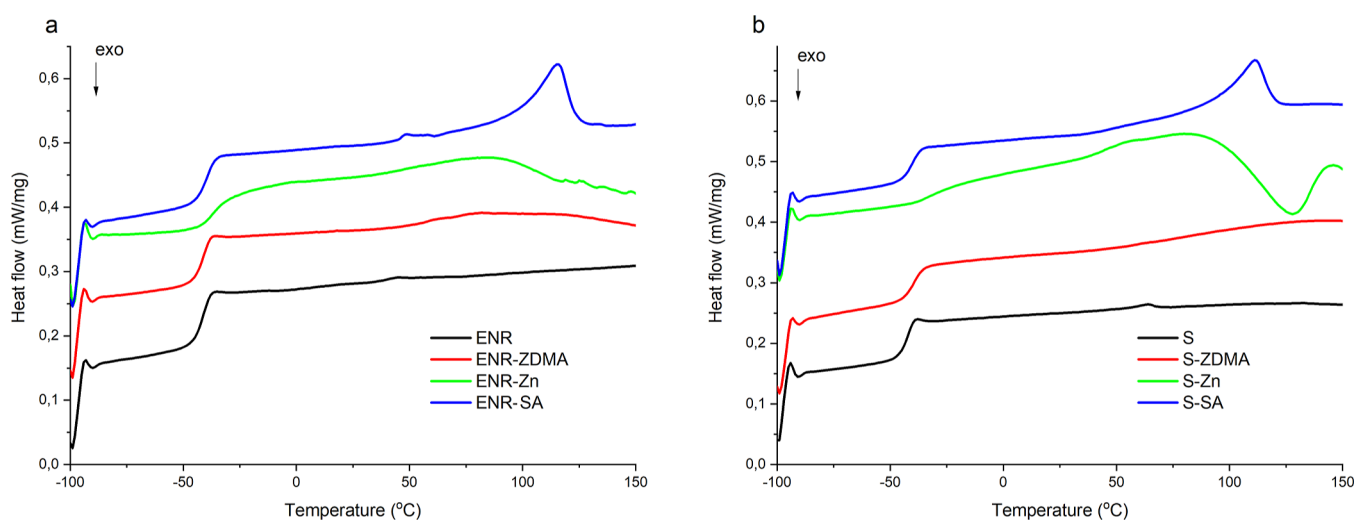
Figure 5. DSC curves of simple compounds (a) without silica and (b) with silica. (Note: curves are shifted along the Y axis for clarity.)

showed the best performance among those. Addition of silica led to an improvement in tensile strength (T_s) and even in ENR alone, which can be related to the good compatibility between silica and ENR as well as the formation of weak physical bonds between them. Among the secondary curatives, both ZDMA and SA had a similar effect on increasing the tensile strength and reducing elongation at break (E_b). However, based on Payne effect measurement data, the mechanisms behind the improvement could be different, and the strength of the S-SA sample should be related to the vulcanization process, while ZDMA-silica network formation would contribute to the tensile strength improvement of S-ZDMA. The poorest mechanical strength and elongation were detected for S-Zn, which could be related to the dominance of the interactions between silica and $ZnCl_2$ rather than between silica-$ZnCl_2$ and silica-ENR, possibly resulting in rigid, short, and brittle bonds, similar to the sacrificial bonds described in ref 53.

The DSC measurements were performed aiming to detect changes in the glass transition temperatures (T_g) and possible transitions related to the presence of secondary curatives. In the DSC curves of the samples with secondary curatives, new peaks appeared above 50 °C, as shown in Figure 5. The broad peak of ENR-Zn and S-Zn above room temperature was most probably related to both the breaking of ionic bonds and the evaporation of bound water from the sample. Some water evaporation from the $ZnCl_2$ containing sample was confirmed by the TGA results (Figure S3 and Table S1), mostly at 100 °C and above, and consisted of two steps, the release of loosely and strongly bound water. These samples also showed the most significant shift in T_g toward higher temperatures

compared to other samples, which was related to the restriction of polymer chain mobility due to short ionic bonds and other interactions between zinc chloride, silica, and elastomer. Although ENR-ZDMA and S-ZDMA samples showed a broad peak at the elevated temperature, neither a notable shift in T_g nor the presence of loosely bound water was noted. The peak is therefore related to the dissociation of weak bonds between the compounding ingredients or the ZDMA particles themselves. Furthermore, ENR-SA and S-SA were the only ones that exhibited clear melting peaks on the DSC curve above 100 °C, thus confirming the previously discussed FTIR data that not all the added SA was consumed during vulcanization.

Effect of Silanes in Simple Compounds. The addition of different silanes is studied in this section, aiming to understand whether the coupling agents facilitate the network built by secondary curatives or restrict it. No change in curing behavior was noted after the addition of ES (Figure S4a), but the shapes of the vulcanization curves changed a little with the addition of TESPT, most likely related to the adsorption of TESPT on the silica surface (Figure S4b). As the rubber compound became more complex with the addition of filler and silanes, FTIR spectra were more difficult to analyze in terms of separate interactions. As can be seen in Figure 6a, addition of silanes to ENR had no significant effect, except for an addition of ES led to a small increase in the peak around 960 cm^{-1}, which could be related either to the stretching vibration of isolated silanol peaks or to C−O vibration.[51,54] Furthermore, FTIR analysis indicated no notable difference between the mentioned simple samples and samples containing ZDMA (Figure 6a,b), except for a minor shift
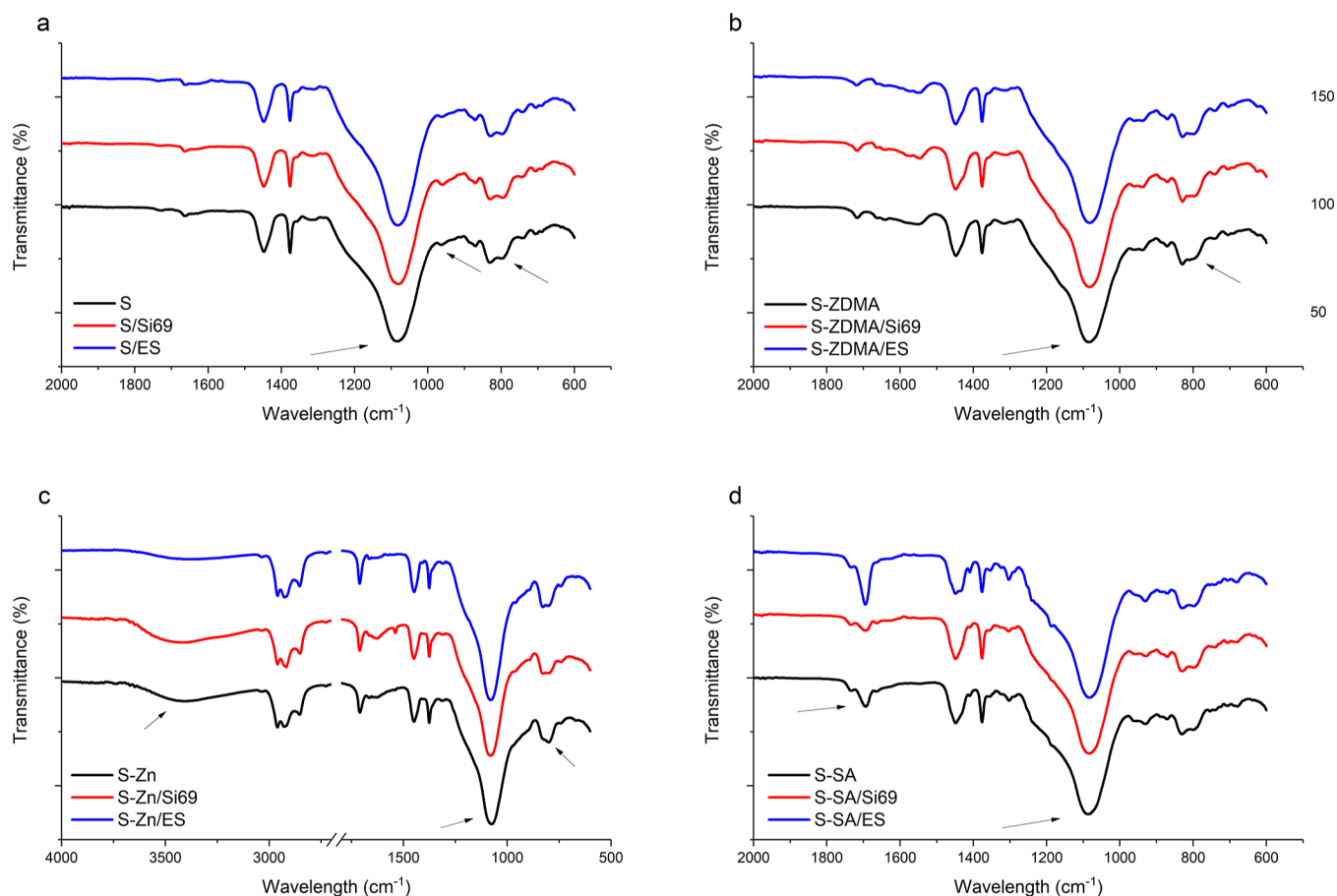
Figure 6. FTIR curves of compounds without conventional curatives with (a) no secondary curative; (b) ZDMA; (c) ZnCl$_2$; and (d) SA. The discussed points of interest are marked with arrows.
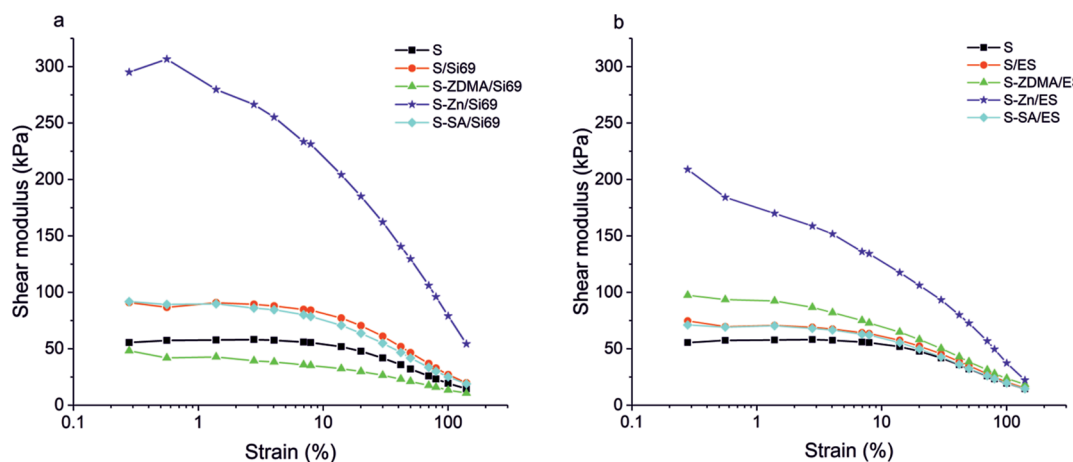

Figure 7. Payne effect in uncured compounds with secondary curatives upon the addition of (a) TESPT and (b) ES coupling agent.

and increase in 1082 and 795 cm^{-1} peaks related to Si–O interactions, suggesting that minor noncovalent interactions may be happening between siloxy-groups and ZDMA. The same results were observed for the rest of the samples as well. Additionally, samples S-Zn/Si69 and S-Zn/ES in Figure 6c had less bound water associated with hygroscopic zinc salt and silica (broad peak around 3300−3400 cm^{-1}) compared to that of S-Zn. It could be suggested that less ZnCl$_2$ was available to adsorb water because of existing interactions with silanes. Otherwise, the FTIR spectra showed no significant changes

between the samples containing zinc chloride. Furthermore, SA was expected to interact with both types of silanes. For example, sample S-SA/ES showed an increased ester bond peak around 1695 cm^{-1} (Figure 6d), which supported the suggestion that SA may react not only with the epoxy group of ENR but also with the epoxy group of ES silane. This type of reaction could create a stronger rubber network.

The effect of the addition of coupling agents supporting the previously discussed results can be seen from the Payne effect measurement data presented in Figure 7. For example, the
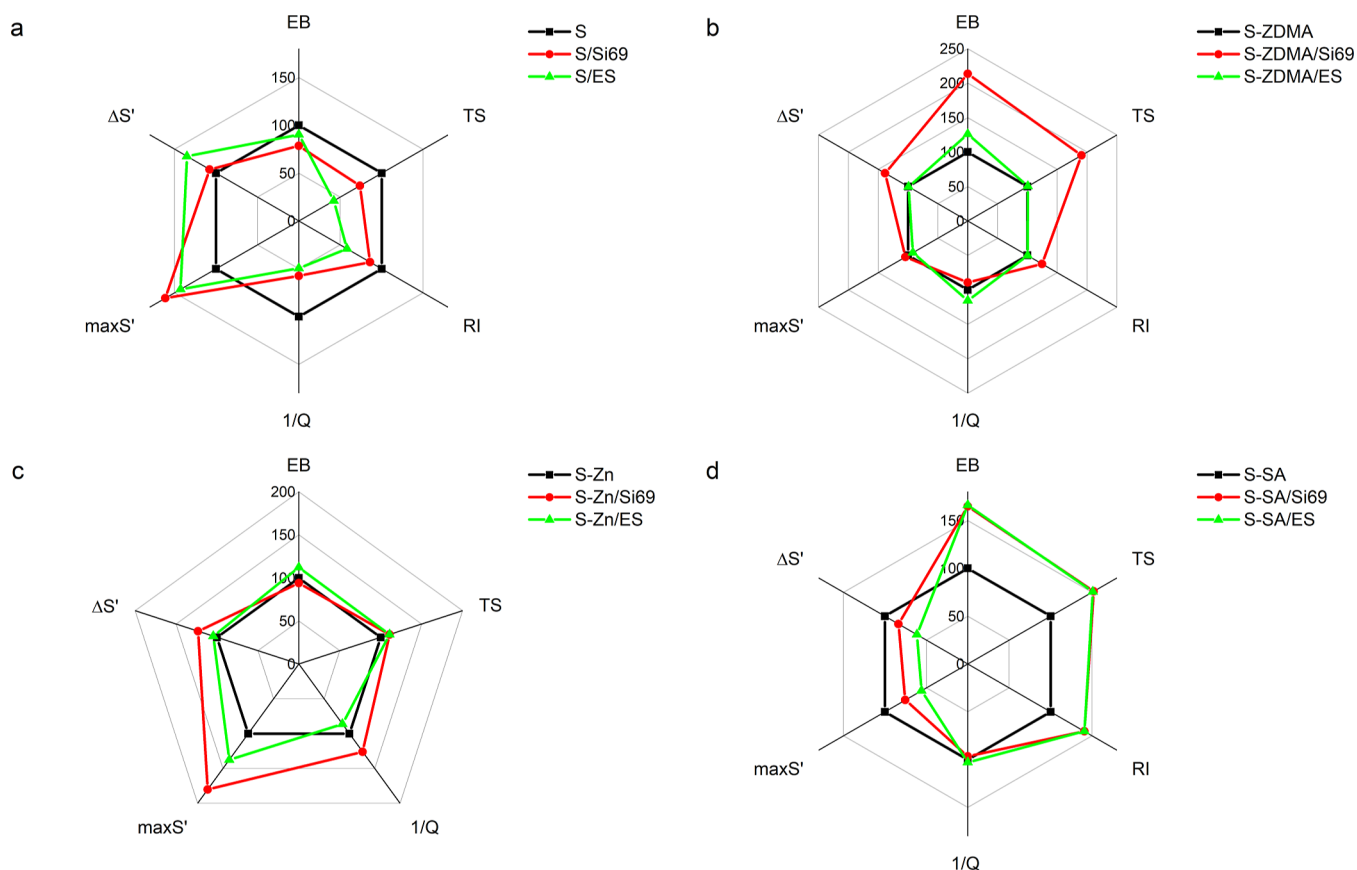
Figure 8. Relative properties of the compounds without conventional curatives with (a) no secondary curatives; (b) ZDMA; (c) ZnCl$_2$; and (d) with SA.

Payne effect was higher for S/Si69 compared to S. This finding supported the evidence of ENR reducing filler−filler interaction in silica more effectively, preventing its agglomeration, and facilitating dispersion compared to TESPT, as mentioned in the work of Sengloyluan et al.[55] The Payne effect of the samples containing SA, as expected, was not affected by the silane type, and the small increase in G'_{min} was related purely to the increase in rubber−filler interactions. Similarly, addition of ZDMA did not lead to a high Payne effect, but the difference between the silanes was more pronounced. As ZDMA seemed to have more interactions with ES than with TESPT, less silane was available for the interaction with silica, which resulted in an increased Payne effect of S-ZDMA/ES. ZnCl$_2$ instead was found to be very active toward all compound ingredients, mostly silica and silanes (especially TESPT), as was also suggested by its tensile properties. Therefore, the Payne effect of such compounds was significantly higher than that of other samples, even before vulcanization.

Finally, Figure 8 shows the relative changes in compound properties with the addition of different types of silanes. The numeric values can be found in Table S2. The addition of coupling agents to ENR resulted in deterioration of tensile properties, RI, and cross-link density but increased torque during curing, possibly related to the hydrodynamic effect and extended filler network formation. The apparent cross-link density of such compounds seemed lower as fewer filler−polymer and polymer−polymer bonds were created when silica reacts with silanes. These findings suggested that silanes may compete with the epoxy group of ENR in reactions with

hydroxy groups of silica, thus creating fewer links between the filler and polymer without the presence of curative. Therefore, these types of silanes cannot be recommended for pure silica-ENR compounds. When secondary curatives are added to the compounds, the interaction mechanisms can become more complicated. ZDMA, however, seemed not to compete with silanes and had some limited interactions with ES. Therefore, the increase in tensile properties and reinforcement seen in Figure 8b was probably related to the parallel independent processes of vulcanization of ENR by ZDMA and ENR−silane−silica interactions. ZnCl$_2$, instead, showed high reactivity toward silica and especially silanes, which could be seen from the airy compound structure (Figure S5a), meaning that components and processing were competing and resulted in no improvement of strength (Figure 8c). As SA may react with epoxy-groups of both ENR and ES silane, a stronger rubber network and enhanced mechanical properties of the compound could be expected, as seen from Figure 8d, when T_s and RI improved significantly. Considering the improvement TESPT brought to the mechanical properties of all samples with secondary curatives and that it is a conventional coupling agent in the rubber industry, further tests were decided to be continued with TESPT, excluding ES.

Effect of the Conventional Curing System. Although the studied secondary curatives could create cross-links in ENR, they were not able to provide the sufficient material properties required for most rubber goods. Therefore, conventional curing systems must be added to optimize the compound properties. According to the curing curves (Figure 9), the addition of secondary curatives had a significant effect
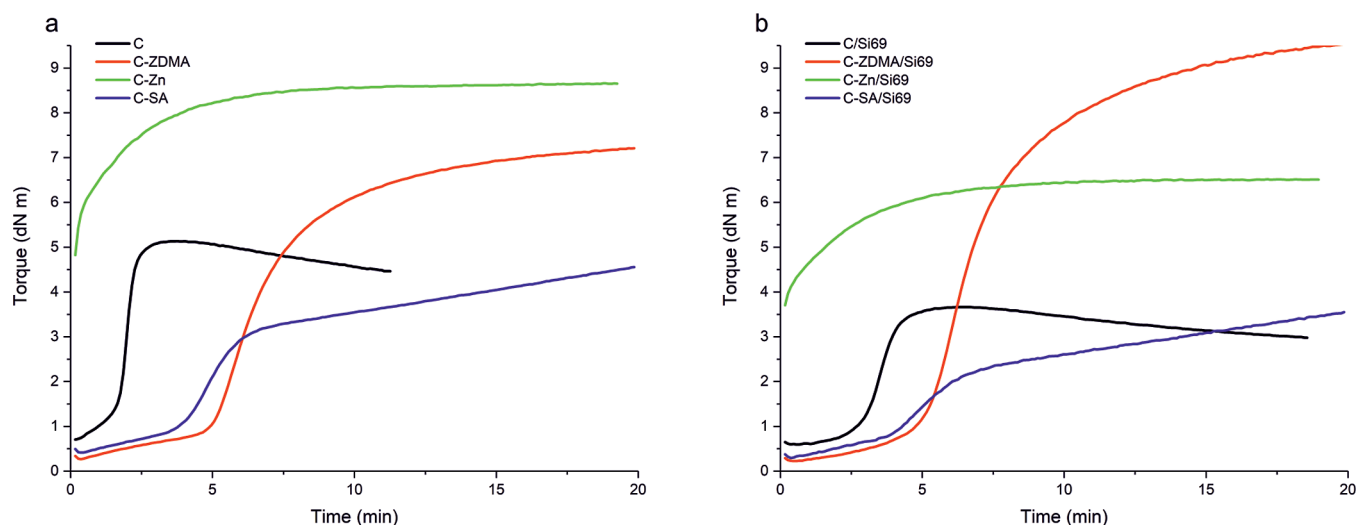
Figure 9. Curing curves of the compounds with conventional curatives (a) without silane and (b) with TESPT silane.
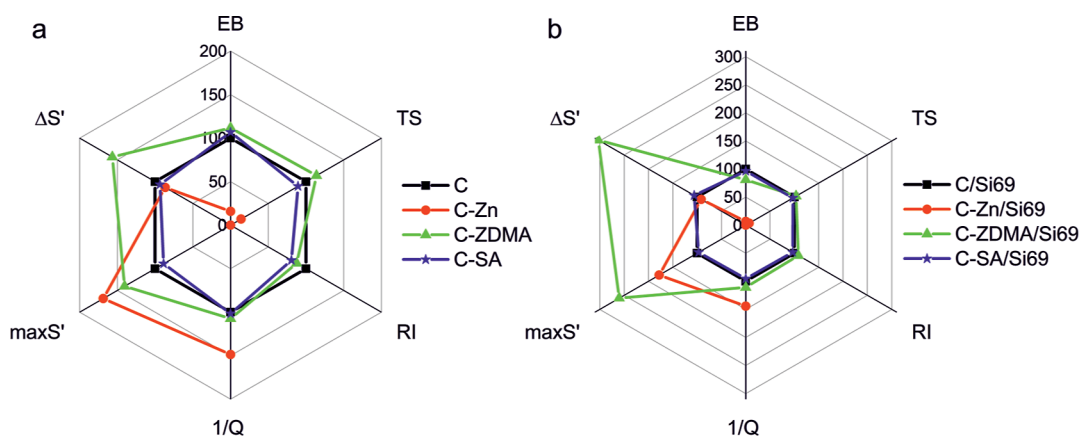

Figure 10. Relative properties of the compounds with conventional curatives (a) without silane and (b) with TESPT silane.

on vulcanization, first, by avoiding reversion (decrease in torque) common for natural rubbers and related to the break-up of polymer chains. Moreover, in the case of samples containing ZDMA and SA, the scorch time increased, and the start of vulcanization was delayed while curing was slower. The smaller increase in torque and generally lower torque values of the samples containing TESPT silane were related to the compatibilizing action of silane and less dense cross-linking, respectively, except for C-ZDMA/Si69, which had the highest torque values (Figure 9b). This was probably related to the effective cross-linking process through separate conventional and secondary curatives simultaneously. For C-SA and C-SA/Si69 samples, curing curves looked like they contained two stages: first, conventional curing, followed by vulcanization with secondary curatives, started at 8−9 min. This could confirm the slow nature of SA and its inability to compete against conventional curatives. Finally, samples containing $ZnCl_2$ had curing curves similar to those of those with only secondary curatives. This suggests that $ZnCl_2$ must fully deactivate conventional curatives, most likely the accelerator, which was later seen in its significantly low tensile properties.

Considering the mechanical properties seen from Figure 10 (numerical values provided in Table S3), only $ZnCl_2$ showed drastic deterioration of tensile strength and elongation at break, while other secondary curatives seemed not to have a

significant effect. This effect supported the previous suggestion about the failure of conventional curatives to create cross-links in the presence of excess $ZnCl_2$. However, the mechanism of such action was unclear. $ZnCl_2$ could possibly react with sulfur and also cause degradation of the CBS accelerator due to its high acidity, especially if some bonded water was involved. Addition of ZDMA had some positive effect on increasing the tensile strength without silane, and SA led to a marginal improvement in T_s in the presence of TESPT.

The cyclic tests indicated that samples containing secondary curatives along with the conventional curing system were prone to some recovery of stress at 200% strain (M_{200}) that could be related to microlevel self-healing phenomena. A similar approach was used in the work of Anyszka et al.[56] to evaluate the reversibility and recovery of silica−polymer bonds. Figure 11 shows that C-SA/Si69 samples were able to regain 95% of M_{200} after 24 h of recovery, and C-ZDMA/Si69 showed the second-best result (81%). At the same time, the C sample had almost no recovery (11%), and C/Si69 exhibited 45% recovery. Samples without silane were generally poorer at regaining M_{200}, and thus, the positive effect of the silane could be confirmed. The effect may be related to the breakdown of silica clusters and the reorganization of chains, providing new reaction sites for silane. Finally, heating was found to be not very effective and could not reach the same level of M_{200} stress
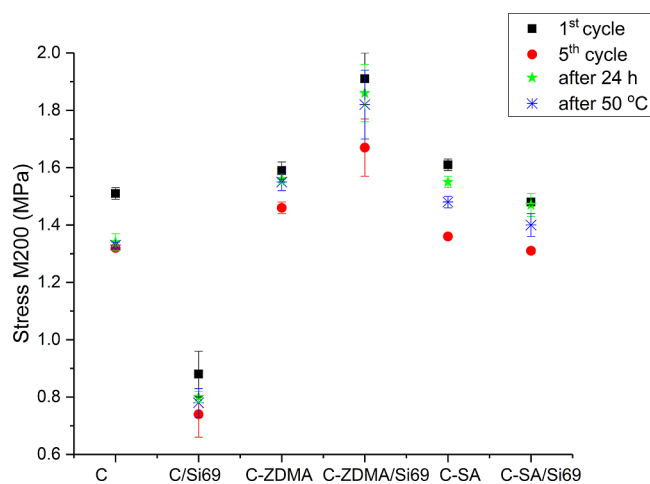
Figure 11. Cyclic testing results expressed in stress at 200% elongation values before and after conditioning.

regain in all of the samples. The samples containing $ZnCl_2$ were not tested cyclically due to their low elongation at break, brittleness, and poor sample quality, such as an uneven grainy surface and blooming on the surface. According to SEM analysis, some bleeding was seen in the samples under vacuum during the sample preparation stage, which can be related to the hydrated and liquified $ZnCl_2$. Potentially, the $ZnCl_2$ load in the sample was too high. It can be speculated that all of the excess zinc salt was leaving the sample and causing blooming (or bleeding) on the surface. Therefore, $ZnCl_2$ amount reduction should be considered. Despite this significant bleeding, the Zn atom distribution within the samples shown by EDS mapping in orange looked uniform but also contained larger zinc agglomerates (Figure 12). Silica, shown in turquoise, was less uniform in distribution in the elastomer phase, forming a cluster-like structure. These clusters are assumed to be silica-rich phases inside the rubber, which could be the result of the compatibilization effect of ENR. Moreover, some voids and silica agglomerates could be seen in the samples containing $ZnCl_2$ in Figure 13a,b. Figure 13c,d indicates that the C-ZDMA and C-SA samples were more uniform and contained no voids.

Effect of $ZnCl_2$ Amount Reduction. The samples containing 10 phr of $ZnCl_2$ showed a significant deterioration of tensile properties and some bleeding, suggesting that the salt load was too high. Therefore, a new set of samples with a

significantly reduced Zn amount was tested. Curing curves indicated that increasing $ZnCl_2$ amount from 0.5 to 2 phr resulted in increasing stiffness of the compounds and progressing marching for S-type compounds, as can be seen from Table 5 data as well. When conventional curatives were added, addition of $ZnCl_2$ reduced reversion of curing and increased scorch time (t_{s2}), as shown in Figure 14b and Table 5, respectively. Furthermore, a significant difference was noted in the shape of curing curves when the zinc salt amount increased from 1 to 2 phr, as seen in Figure 14. This could suggest that the conventional curatives were deactivated by $ZnCl_2$ when the amount of zinc salt exceeded the amount of sulfur or accelerator. These changes could be related to the polymer chain scission by the reaction products between secondary and conventional curatives. Another possible route is that the presence of conventional curatives, especially sulfur, and surface-bonded water promoted chlorination of ENR, thus leading to both a reduction of zinc available for cross-linking and a curing system incapable of curing such samples.[23] Potentially, the addition of a small amount of ZnO in the final mixing stage could improve the vulcanization behavior and final tensile properties of the compound.

Considering the compound properties, addition of $ZnCl_2$ without conventional curatives resulted in a gradual decrease of elongation at break and an increase in cross-link density and RI. Furthermore, a high deviation in tensile strength between the parallel samples could be noted, meaning the mixing was not efficient in dispersing zinc salt. When the conventional curing system was added, an even more significant decrease in elongation at break and tensile strength was seen after $ZnCl_2$ content exceeded 0.5 phr. The results may be explained by the domination of short and rigid zinc induced bonds over more flexible sulfur bonds.

According to the Payne effect measurements, the addition of conventional curatives had a marginal effect on ENR without secondary curatives (Figure 15), but the effect of $ZnCl_2$ addition was more pronounced, especially for C-type samples containing a conventional curing system. As seen in Figure 15b, the Payne effect increased gradually with the increasing amount of $ZnCl_2$. The difference between S-type and C-type samples could be explained by better zinc salt distribution due to the prolonged mixing associated with the addition of conventional curatives. Soon as the difference in Payne effect was already seen with 0.5 phr $ZnCl_2$, which was not enough to
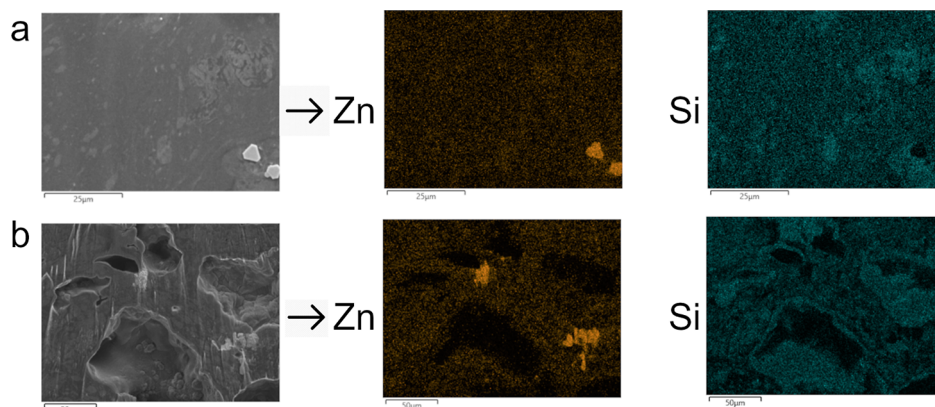
Figure 12. SEM pictures and EDS mapping of (a) S-Zn and (b) C-Zn samples. Zn is shown in orange, and Si is shown in cyan.
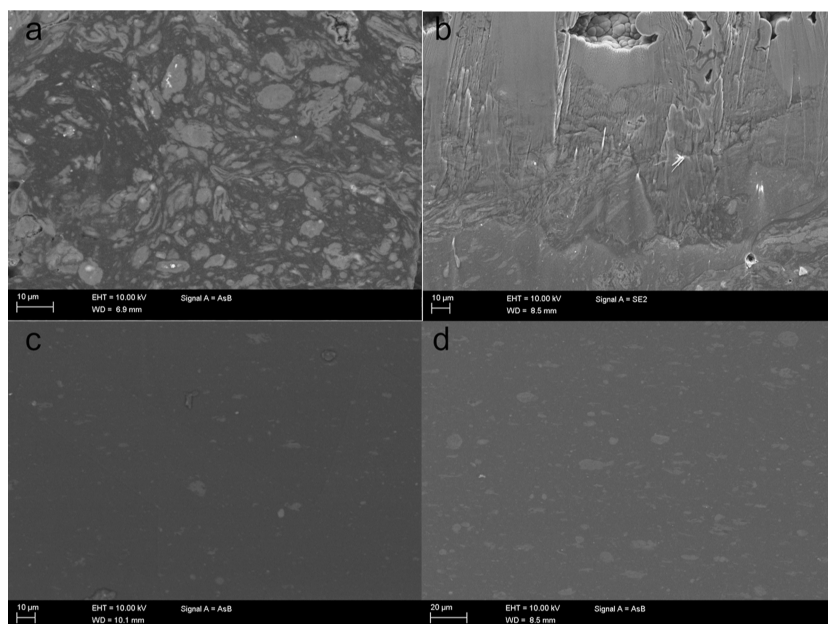
Figure 13. SEM pictures of (a) S-Zn, (b) C-Zn, (c) C-ZDMA, and (d) C-SA.

Table 5. Properties of the Compounds with a Reduced $ZnCl_2$ Amount with and without Conventional Curatives

| sample	t_{s2}, min	$\Delta S'$, dN m	S'_{max}, dN m	T_s, MPa	E_b, %	M_{100}, MPa	M_{300}, MPa	RI, —	$1/Q$, g/g
S		0.324	0.846	4.23 ± 0.40	512.1 ± 26.3	0.85 ± 0.03	2.35 ± 0.16	2.77 ± 0.09	0.095 ± 0.004
S-Zn0.5		0.638	1.746	3.76 ± 0.45	439.5 ± 28.5	0.92 ± 0.05	2.36 ± 0.13	2.56 ± 0.02	0.097 ± 0.002
S-Zn1		0.629	1.879	3.54 ± 0.65	376.6 ± 64.9	1.03 ± 0.02	2.69 ± 0.01	2.62 ± 0.05	0.110 ± 0.007
S-Zn2		1.074	2.434	4.21 ± 0.11	318.6 ± 6.8	1.27 ± 0.01	3.92 ± 0.11	3.07 ± 0.05	0.142 ± 0.002
C	1.93	4.530	5.138	16.41 ± 5.38	476.2 ± 86.7	1.56 ± 0.05	6.77 ± 0.14	4.35 ± 0.07	0.255 ± 0.004
C-Zn0.5	5.87	4.391	5.068	15.40 ± 1.82	415.6 ± 47.2	1.73 ± 0.02	8.20 ± 0.25	4.73 ± 0.09	0.254 ± 0.033
C-Zn1	6.51	4.899	5.758	10.24 ± 4.28	286.1 ± 64.1	2.25 ± 0.05			0.267 ± 0.005
C-Zn2	10.57	2.952	3.827	6.60 ± 0.51	262.1 ± 7.7	1.86 ± 0.1			0.294 ± 0.009
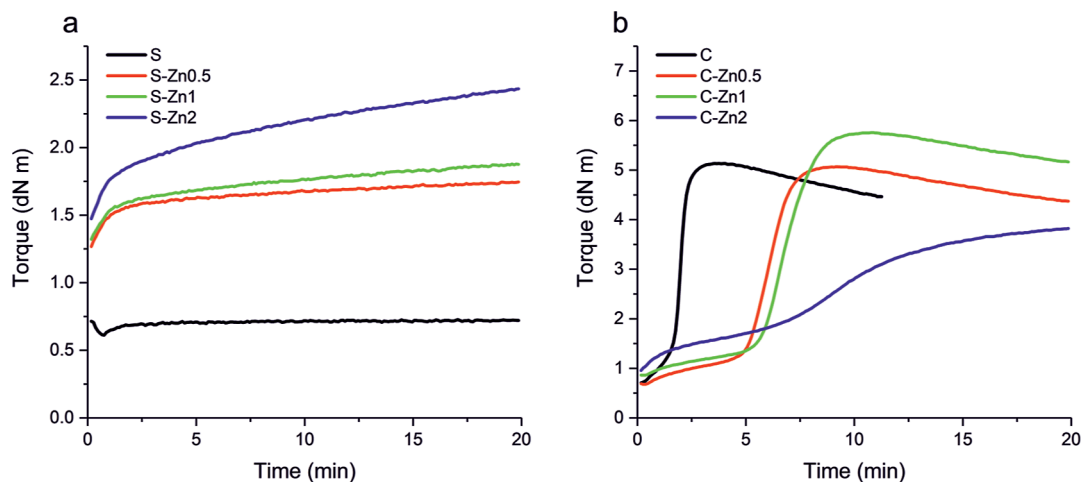
Figure 14. Curing curves of the compounds with reduced $ZnCl_2$ amount (a) without conventional curatives and (b) with conventional curatives.

create a filler network along, the effect could reflect the weak secondary network created with the assistance of Zn^{2+} ions.

Cyclic testing of the samples containing reduced amounts of $ZnCl_2$ and conventional curatives revealed that stress recovery reached its maximum with a 1 phr concentration of zinc salt (Figure 16). This compound showed full recovery of M_{200} of the samples kept for 24 h in ambient conditions between the tests. Moreover, M_{200} at the fifth cycle after 24 h of

conditioning increased, while for reference C, the stress was reduced even further. As previously discussed, heat did not lead to a similar stress recovery.

■ CONCLUSIONS

The findings suggest that Payne effect measurements of both cured and uncured samples can be used for the evaluation of short and weak sacrificial bonds in a similar way they are used
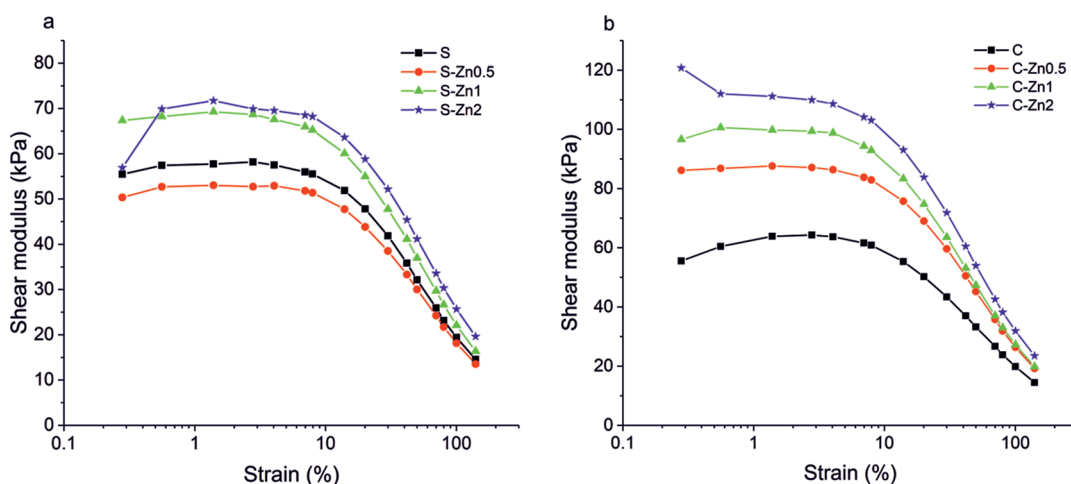
Figure 15. Payne effect of the compounds with reduced $ZnCl_2$ amount (a) without conventional curatives and (b) with conventional curatives.
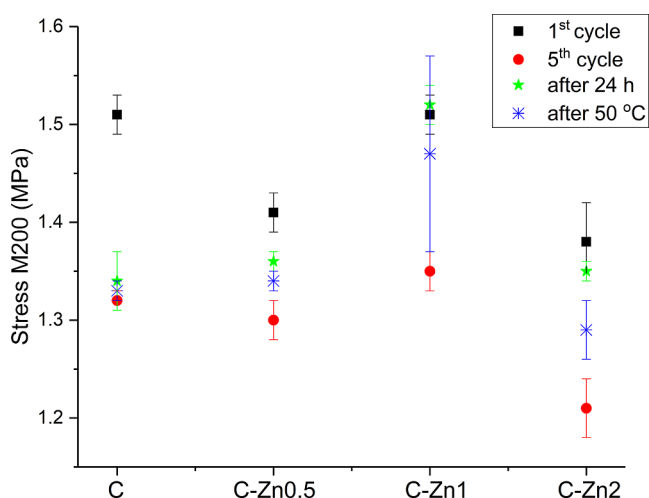
Figure 16. Cyclic test results of the samples with a reduced Zn amount.

for the study of filler−filler interactions. Among the studied secondary curatives, ZDMA showed the improvement of tensile properties and some microscale self-healing after the cyclic load; it was also found to interfere with the traditional curatives the least. Although the addition of dicarboxylic acid led to a similar self-healing effect, it marginally decreased the tensile properties of the compounds. The addition of 10 phr $ZnCl_2$ to the rubber led to significant deterioration of the tensile properties, restricted conventional vulcanization, and showed the ability to create weak and brittle, potentially sacrificial, bonds with ENR. This combination of materials could possibly be used to create a sacrificial network when mixed with other rubber types and should be a topic of further investigation, including the optimization of compound ingredients, mixing, and vulcanization parameters, as well as addressing stability and durability. If to be used with ENR, the amount of $ZnCl_2$ should be reduced below the amount of the traditional curing system, and in the present study, 1 phr $ZnCl_2$ could be considered optimum. For example, such a compound showed full stress recovery after cyclic testing and had fair tensile properties compared to the reference. Possible applications of the compounds containing secondary curatives can include rubber goods undergoing periodic cyclic loading,

for example, in robotics, specialized conveyor belts, or tire components.

ASSOCIATED CONTENT

Supporting Information

The Supporting Information is available free of charge at https://pubs.acs.org/doi/10.1021/acsomega.4c03271.

> Chemical structures of the materials used in the study and visual differences of cured samples and the structure of S-type compounds after the mixing stage, TGA curves, and numerical data of the selected samples, numerical data for Figures 8 and 10, and some additional curing curves (PDF)

AUTHOR INFORMATION

Corresponding Author

Essi Sarlin − *Materials Science and Environmental Engineering, Tampere University, FI-33014 Tampere, Finland;* orcid.org/0000-0002-2525-9639; Email: essi.sarlin@tuni.fi

Authors

Alexandra Shakun − *Materials Science and Environmental Engineering, Tampere University, FI-33014 Tampere, Finland; Nokian Tyres plc, FI-37101 Nokia, Finland*

Noora Kemppainen − *Nokian Tyres plc, FI-37101 Nokia, Finland*

Complete contact information is available at: https://pubs.acs.org/10.1021/acsomega.4c03271

Notes

The authors declare no competing financial interest.

ACKNOWLEDGMENTS

■ REFERENCES

(1) Zhou, X.; Guo, B.; Zhang, L.; Hu, G.-H. Progress in bio-inspired sacrificial bonds in artificial polymeric materials. *Chem. Soc. Rev.* **2017**, *46* (20), 6301−6329.

(2) Boonmahitthisud, A.; Boonkerd, K. Sustainable development of natural rubber and its environmentally friendly composites. *Curr. Opin. Green Sustainable Chem.* **2021**, *28*, 100446.

(3) Araujo-Morera, J.; Verdejo, R.; López-Manchado, M. A.; Hernández Santana, M. Sustainable mobility: The route of tires through the circular economy model. *Waste Manag.* **2021**, *126*, 309−322.

(4) Olthuis, M., Relevance and development of new rubber technology competences for a sustainable automotive industry. 2020. http://essay.utwente.nl/81382/ (accessed on Nov 17, 2023).

(5) Utrera-Barrios, S.; Steenackers, N.; Terryn, S.; Ferrentino, P.; Verdejo, R.; Van Asche, G.; López-Manchado, M. A.; Brancart, J.; Hernández Santana, M. Unlocking the potential of self-healing and recyclable ionic elastomers for soft robotics applications. *Mater. Horiz.* **2024**, *11* (3), 708−725.

(6) Wang, W.; Wang, W.; Wang, F.; Xie, X.; Yi, G.; Li, Z. Tough and body-temperature self-healing polysiloxane elastomers through building a double physical crosslinking network via competing noncovalent interactions. *J. Mater. Chem. A* **2022**, *10* (43), 23375−23383.

(7) Cheng, B.; Lu, X.; Zhou, J.; Qin, R.; Yang, Y. Dual Cross-Linked Self-Healing and Recyclable Epoxidized Natural Rubber Based on Multiple Reversible Effects. *ACS Sustain. Chem. Eng.* **2019**, *7* (4), 4443−4455.

(8) Cheng, Z.; Yan, M.; Cao, L.; Huang, J.; Cao, X.; Yuan, D.; Chen, Y. Design of Nitrile Rubber with High Strength and Recycling Ability Based on Fe3+-Catechol Group Coordination. *Ind. Eng. Chem. Res.* **2019**, *58* (9), 3912−3920.

(9) Jia, Z.; Zhu, S.; Chen, Y.; Zhang, W.; Zhong, B.; Jia, D. Recyclable and self-healing rubber composites based on thermoreversible dynamic covalent bonding. *Composites, Part A* **2020**, *129*, 105709.

(10) Polgar, L. M.; van Duin, M.; Broekhuis, A. A.; Picchioni, F. Use of Diels-Alder Chemistry for Thermoreversible Cross-Linking of Rubbers: The Next Step toward Recycling of Rubber Products? *Macromolecules* **2015**, *48*, 7096−7105.

(11) Xiang, H. P.; Rong, M. Z.; Zhang, M. Q. Self-healing, Reshaping, and Recycling of Vulcanized Chloroprene Rubber: A Case Study of Multitask Cyclic Utilization of Cross-linked Polymer. *ACS Sustain. Chem. Eng.* **2016**, *4* (5), 2715−2724.

(12) Xu, C.; Huang, X.; Li, C.; Chen, Y.; Lin, B.; Liang, X. Design of 'Zn2+ Salt-Bondings' Cross-Linked Carboxylated Styrene Butadiene Rubber with Reprocessing and Recycling Ability via Rearrangements of Ionic Cross-Linkings. *ACS Sustain. Chem. Eng.* **2016**, *4* (12), 6981−6990.

(13) Sánchez, M. C.; García, D. B.; Escobar, M. M.; Mansilla, M. Self-Healable Elastomers. In *Self-Healing Smart Materials and Allied Applications*; John Wiley & Sons, Ltd, 2021; pp 65−97..

(14) Hernández Santana, M.; den Brabander, M.; García, S.; van der Zwaag, S. Routes to Make Natural Rubber Heal: A Review. *Polym. Rev.* **2018**, *58* (4), 585−609.

(15) Utrera-Barrios, S.; Verdejo, R.; López-Manchado, M. A.; Hernández Santana, M. Evolution of self-healing elastomers, from extrinsic to combined intrinsic mechanisms: a review. *Mater. Horiz.* **2020**, *7* (11), 2882−2902.

(16) Huang, J.; Zhang, L.; Tang, Z.; Guo, B. Bioinspired engineering of sacrificial bonds into rubber networks towards high-performance and functional elastomers. *Compos. Commun.* **2018**, *8*, 65−73.

(17) Neal, J.; Mozhdehi, D.; Guan, Z. Enhancing Mechanical Performance of a Covalent Self-Healing Material by Sacrificial Non-Covalent Bonds. *J. Am. Chem. Soc.* **2015**, *137*, 4846−4850.

(18) Chumnum, K.; Kalkornsurapranee, E.; Johns, J.; Sengloyluan, K.; Nakaramontri, Y. Combination of Self-Healing Butyl Rubber and Natural Rubber Composites for Improving the Stability. *Polymers* **2021**, *13* (3), 443.

(19) Mandal, S.; Das, A.; Euchler, E.; Wiessner, S.; Heinrich, G.; Sawada, J.; Matsui, R.; Nagase, T.; Tada, T. Dynamic reversible networks and development of self-healing rubbers: a critical review. *Rubber Chem. Technol.* **2023**, *96* (2), 175−195.

(20) Najwa Thajudin, N. L.; Zainol, M.; Khimi, R. Intrinsic room temperature self-healing natural rubber based on metal thiolate ionic network. *Polym. Test.* **2021**, *93*, 106975.

(21) Wu, M.; Yang, L.; Shen, Q.; Zheng, Z.; Xu, C. Endeavour to balance mechanical properties and self-healing of nature rubber by increasing covalent crosslinks via a controlled vulcanization. *Eur. Polym. J.* **2021**, *161*, 110823.

(22) Fueangphakdee, P.; Nimpaiboon, A.; Junkong, P. Protein-Mediated ZnO Synthesis for Self-Healing in Natural Rubber. *Macromol. Mater. Eng.* **2024**, *309* (4), 2300406.

(23) Damampai, K.; Pichaiyut, S.; Mandal, S.; Wießner, S.; Das, A.; Nakason, C. Internal Polymerization of Epoxy Group of Epoxidized Natural Rubber by Ferric Chloride and Formation of Strong Network Structure. *Polymers* **2021**, *13* (23), 4145.

(24) Gong, Z.; Huang, J.; Cao, L.; Xu, C.; Chen, Y. Self-healing epoxidized natural rubber with ionic/coordination crosslinks. *Mater. Chem. Phys.* **2022**, *285*, 126063.

(25) Jiang, C.; He, H.; Yao, X.; Yu, P.; Zhou, L.; Jia, D. Self-crosslinkable lignin/epoxidized natural rubber composites. *J. Appl. Polym. Sci.* **2014**, *131* (23), 41166.

(26) Pire, M.; Norvez, S.; Iliopoulos, I.; Le Rossignol, B.; Leibler, L. Epoxidized natural rubber/dicarboxylic acid self-vulcanized blends. *Polymer* **2010**, *51* (25), 5903−5909.

(27) Rahman, M. A.; Sartore, L.; Bignotti, F.; Di Landro, L. Autonomic Self-Healing in Epoxidized Natural Rubber. *ACS Appl. Mater. Interfaces* **2013**, *5* (4), 1494−1502.

(28) Zhang, X.; Lin, T.; Tang, Z.; Guo, B. Elastomeric Composites based on Zinc Diacrylate-Cured Epoxidized Natural Rubber: Mechanical Properties and Ageing-Resistance. *KGK Rubberpoint* **2015**, *68* (7−8), 39−45.

(29) Blume, A.; Kaewsakul, W.; Sahakaro, K.; Dierkes, W. K.; Noordermeer, J. W. M., Interactions between Silica and Epoxidized Natural Rubber with and without Silane. *Proceedings of 186th Technical Meeting ACS Rubber Division*; ACS Rubber Division: Nashville, TN, USA, Oct 2014; pp 1−12.

(30) Kaewsakul, W.; et al. 9 - Natural rubber and epoxidized natural rubber in combination with silica fillers for low rolling resistance tires. In *Chemistry, Manufacture, and Application of Natural Rubber*, 2nd ed.; Kohjiya, S., Ikeda, Y., Eds.; Woodhead Publishing in Materials, Woodhead Publishing, 2021; pp 247−316..

(31) Martin, P. J.; Brown, P.; Chapman, A. V.; Cook, S. Silica-reinforced epoxidized natural rubber tire treads — performance and durability. *Rubber Chem. Technol.* **2015**, *88* (3), 390−411.

(32) Ogunsona, E. O.; Misra, M.; Mohanty, A. K. Influence of epoxidized natural rubber on the phase structure and toughening behavior of biocarbon reinforced nylon 6 biocomposites. *RSC Adv.* **2017**, *7* (15), 8727−8739.

(33) Ryu, G.; Kim, D.; Song, S.; Hwang, K.; Ahn, B.; Kim, W. Effect of Epoxide Content on the Vulcanizate Structure of Silica-Filled Epoxidized Natural Rubber (ENR) Compounds. *Polymers* **2021**, *13* (11), 1862.

(34) Sengloyluan, K.; Sahakaro, K.; Dierkes, W. K.; Noordermeer, J. W. M. Silica-reinforced tire tread compounds compatibilized by using epoxidized natural rubber. *Eur. Polym. J.* **2014**, *51* (1), 69−79.

(35) Varughese, S.; Tripathy, D. K. Chemical interaction between epoxidized natural rubber and silica: Studies on cure characteristics and low-temperature dynamic mechanical properties. *J. Appl. Polym. Sci.* **1992**, *44* (10), 1847−1852.

(36) Xu, T.; Jia, Z.; Luo, Y.; Jia, D.; Peng, Z. Interfacial interaction between the epoxidized natural rubber and silica in natural rubber/silica composites. *Appl. Surf. Sci.* **2015**, *328*, 306−313.

(37) Canadell, J.; Goossens, H.; Klumperman, B. Self-Healing Materials Based on Disulfide Links. *Macromolecules* **2011**, *44* (8), 2536−2541.

(38) Low, D. Y. S.; Supramaniam, J.; Leong, W.; Soottitantawat, A.; Charinpanitkul, T.; Tanthapanichakoon, W.; Manickam, S.; Tan, K.; Goh, B.; Tang, S. Self-healing synthetic rubber composites: review of recent progress and future directions towards sustainability. *Mater. Today Sustain.* **2023**, *24*, 100545.

(39) Araujo-Morera, J.; López-Manchado, M. A.; Verdejo, R.; Hernández Santana, M. Unravelling the effect of healing conditions and vulcanizing additives on the healing performance of rubber networks. *Polymer* **2022**, *238*, 124399.

(40) Li, Q.; Zhao, S.; Pan, Y. Structure, morphology, and properties of HNBR filled with N550, SiO2, ZDMA, and two of three kinds of fillers. *J. Appl. Polym. Sci.* **2010**, *117* (1), 421−427.

(41) Zhang, X. H.; Tang, Z. H.; Huang, J.; Lin, T. F.; Guo, B. C. Strikingly Improved Toughness of Nonpolar Rubber by Incorporating Sacrificial Network at Small Fraction. *J. Polym. Sci., Part B: Polym. Phys.* **2016**, *54* (8), 781−786.

(42) Lin, T.; Guo, B. Curing of Rubber via Oxa-Michael Reaction toward Significantly Increased Aging Resistance. *Ind. Eng. Chem. Res.* **2013**, *52* (51), 18123−18130.

(43) Wang, H.; Liu, W.; Huang, J.; Yang, D.; Qiu, X. Bioinspired Engineering towards Tailoring Advanced Lignin/Rubber Elastomers. *Polymers* **2018**, *10* (9), 1033.

(44) Chen, Y.; Tang, Z.; Liu, Y.; Wu, S.; Guo, B. Mechanically Robust, Self-Healable, and Reprocessable Elastomers Enabled by Dynamic Dual Cross-Links. *Macromolecules* **2019**, *52* (10), 3805−3812.

(45) Montarnal, D.; Capelot, M.; Tournilhac, F.; Leibler, L. Silica-Like Malleable Materials from Permanent Organic Networks. *Science* **2011**, *334* (6058), 965−968.

(46) Abraham, T. W.; Höfer, R. Volume 10: Polymers for a Sustainable Environment and Green Energy. *Polymer Science: A Comprehensive Reference*; Elsevier: Amsterdam, 2012; pp 15−58.

(47) Harun, F.; Chan, C. H. *Electronic Applications of Polymer Electrolytes of Epoxidized Natural Rubber and Its Composites*; Springer, 2016; pp 37−59..

(48) Rolere, S.; Liengprayoon, S.; Vaysse, L.; Sainte-Beuve, J.; Bonfils, F. Investigating natural rubber composition with Fourier Transform Infrared (FT-IR) spectroscopy: A rapid and non-destructive method to determine both protein and lipid contents simultaneously. *Polym. Test.* **2015**, *43*, 83−93.

(49) Zhao, M.; Chen, H.; Yuan, J.; Wu, Y.; Li, S.; Liu, R. The study of ionic and entanglements self-healing behavior of zinc dimethacrylate enhanced natural rubber and natural rubber/butyl rubber composite. *J. Appl. Polym. Sci.* **2022**, *139* (17), 52048.

(50) Gong, C.; Cao, J.; Guo, M.; Cai, S.; Xu, P.; Lv, J.; Li, C. A facile strategy for high mechanical performance and recyclable EPDM rubber enabled by exchangeable ion crosslinking. *Eur. Polym. J.* **2022**, *175*, 111339.

(51) Coates, J. Interpretation of Infrared Spectra, A Practical Approach. *Encyclopedia of Analytical Chemistry*, Book, Section vols.; John Wiley & Sons, Ltd, 2006..

(52) Litvinov, M. V.; De, P. P. Application of infrared spectroscopy to characterise chemically modified rubbers and rubbery materials. *Spectroscopy of Rubber and Rubbery Materials*; Smithers Rapra Technology Ltd, 2002; pp 125−165.

(53) Nakajima, T. Generalization of the sacrificial bond principle for gel and elastomer toughening. *Polym. J.* **2017**, *49* (6), 477−485.

(54) Courtney, T. D.; Chang, C.-C.; Gorte, R. J.; Lobo, R. F.; Fan, W.; Nikolakis, V. Effect of water treatment on Sn-BEA zeolite: Origin of 960 cm−1 FTIR peak. *Microporous Mesoporous Mater.* **2015**, *210*, 69−76.

(55) Sengloyluan, K.; Sahakaro, K.; Dierkes, W. K.; Noordermeer, J. W. M. Synergistic Effects in Silica-Reinforced Natural Rubber Compounds Compatibilised by ENR in Combination with Different Silane Coupling Agent Types. *J. Rubber Res.* **2016**, *19* (3), 170−189.

(56) Anyszka, R.; Beton, K.; Szczechowicz, M.; Bielinski, D. M.; Blume, A. Velcro-inspired supramolecular system for silica-rubber coupling. *Rubber Chem. Technol.* **2020**, *93* (4), 672−682.